

Article

# Exploration of structural mechanics and biomimetic design in sculpture art creation

Jing Guo, Jinxiu Zu\*

School of Physical Education and Art, Caofeidian Vocational and Technical College, Tangshan 199010, China

\* **Corresponding author:** Jinxiu Zu, 18932525986@163.com

## CITATION

Guo J, Zu J. Exploration of structural mechanics and biomimetic design in sculpture art creation. *Molecular & Cellular Biomechanics*. 2025; 22(3): 1131.  
<https://doi.org/10.62617/mcb1131>

## ARTICLE INFO

Received: 17 December 2024  
Accepted: 8 January 2025  
Available online: 13 February 2025

## COPYRIGHT



Copyright © 2025 by author(s).  
*Molecular & Cellular Biomechanics* is published by Sin-Chn Scientific Press Pte. Ltd. This work is licensed under the Creative Commons Attribution (CC BY) license.  
<https://creativecommons.org/licenses/by/4.0/>

**Abstract:** With the development of economy, the public's demand for cultural life is increasing. Sculpture brings a dynamic experience to the urban landscape, enabling people to actively participate and integrate into the landscape space, thus adding to the urban cultural construction and enhancing the variability and depth of space. Based on the principle of bionic design, this paper compares the degree of similarity of the original organisms, and divides the morphology bionic into figurative bionic, abstract bionic, and metaphorical bionic. Combined with the structural stress characteristics, the spatial finite element model is established, and according to D'Alembert's principle, the vibration equilibrium equation is associated, and the vibration mode superposition method power analysis method is applied to analyze the modal state of a sculpture. The results show that: The horizontal direction of the vibration mode coefficient has reached more than 0.9, the period and frequency of the sixth and seventh order vibration modes are the same, both are 0.3948 s and 2.5699 Hz. Calculating the ultimate bearing capacity of the structure under all the conditions, the maximum stress ratio of the strength of each member of the sculpture is 0.96987, which indicates that the strength of all the structural members meets the requirements of the design of the sculpture. The overall stability of the sculpture is analyzed, when the order is 5, the buckling factor under three kinds of loading conditions are 208.5974, 114.1648, 124.9748, which indicates that the sculpture structure designed according to bionics has good overall stability.

**Keywords:** bionic design; spatial finite element model; D'Alembert's principle; vibration superposition method dynamic analysis; sculpture design

## 1. Introduction

The rapid development of Chinese society and economy has promoted the vigorous development of art, and the creation of sculpture art has also had a personalized development trend. Sculpture is a kind of composite level art form, combining three-dimensional and semi-dimensional and other levels, fully reflecting the material form of cultural nature [1,2]. Artists will fully select and utilize diverse cultural elements such as different materials, tools, production techniques and post-production modeling treatments, placing places, etc., so that the art works can have a more unique presentation [3–5].

With the development of human material civilization, people engaged in social activities and production construction need to build large sculpture structures to meet practical and aesthetic requirements. As a typical heterogeneous space plate and shell structure, the sculpture structure is characterized by irregularity, self-importance, and miscellaneous forces [6,7]. Therefore, it is necessary to analyze the mechanical properties of such shaped space plate structures in order to ensure the safety and durability requirements for the use of the structure [8,9].

In addition, the concept of biomimicry is the most important source of inspiration for people since primitive society, and the colorful and complex nature has always attracted people to imitate and learn from it, and the creation of sculpture art is a typical example of this. Bionic art is not directly displaying or placing living organisms in art works, but a type of art that works by transforming and creating life from a biological perspective [10–12]. From the perspective of bionics, the disciplinary theories, ideologies, and technological achievements of bionics have provided more possibilities for the creation of sculpture art [13]. On the one hand, artists draw inspiration from nature and apply bionic concepts to art creation to enrich their art form language [14–16]. On the other hand, the products of bionic technology are integrated into their art form language to provide bionic technology support for art [17–19]. Based on this, sculpture art connects the concept of nature through bionics with the viewer through art works, enriching the viewer's aesthetic experience while also conveying the artistic concept of nature.

This paper proposes a method of creating sculpture art that is designed to resemble the principle characteristics of biological systems according to the form and working principle of living organisms. The external characteristics of natural creatures and their symbolism are applied to sculpture design through artistic methods, according to different design principles, providing new ideas for the innovative application of bionic design in sculpture. The structural system of the statue is constructed, and the horizontal lateral shift of the structure is considered as the focus of the structural design, for which the spatial finite element structural model is established. Based on D'Alembert's principle, the free vibration equations are expressed in matrix form through the coupled equations. In the modal analysis of a sculpture, the first 100 order vibration modes are calculated, and the structural mechanical state of the sculpture based on bionic design is analyzed from the seismic effect, component stress calculation, overall stability and force condition to verify the feasibility of this method.

## **2. Sculpture art creation under the view of biomimicry**

### **2.1. Bionic design**

Bionic design science, also called design bionics, is a cross-discipline developed on the basis of bionics and design science [20]. Bionic design science is a new design thinking method through the experimental simulation of certain principles of biological systems, which is organized, analyzed, and then refined, so as to design a new design thinking method that resembles the characteristics of the principles of biological systems. In the field of design, bionic design has become a research hotspot. People design products with vivid appearance, easy operation and powerful functions according to the form and working principle of living organisms, such as gliders made by simulating the movement of birds' wings. The history of the development of human artifacts is the process of constantly drawing inspiration from nature.

### **2.2. Application of bionic design in sculpture**

#### **2.2.1. Morphological bionics**

Morphological biomimicry design applies the external characteristics of natural organisms and their symbolism to the design through artistic methods, and can be divided into figurative biomimicry, abstract biomimicry and metaphorical biomimicry to differentiate the degree of similarity of design outputs compared with the original organisms.

(1) Figurative Bionics

Figurative biomimicry refers to the fact that the design outputs are closer to the natural objects in terms of appearance and form, and the viewers can easily recognize the natural objects with the characteristics of the form. In daily life, the figurative form of the design has a richer naturalness, affinity and sense of fun.

(2) Abstract Bionic

Abstract biomimicry uses the abstract form of natural objects, which starts from the specific natural objects, and is the artistic image obtained by the designer after summarizing the characteristics of the creatures. Different designers of the same natural object generalization presents different forms of expression, which is benevolent, wise and wise. Abstract biomimicry designer's own abstract generalization ability is unique and exploratory, and the form and performance of the movement of the work also leave the viewer a certain space for imagination.

(3) Metaphorical Biomimicry

Metaphorical bionic use of metaphor, symbolism, the use of certain attributes of natural objects to express the characteristics of dynamic sculpture. What the creator wants to express is the cycle of change of natural things, and the work contains certain philosophical concepts, i.e., the concept of the cycle of change.

### **2.2.2. Functional bionics**

Functional bionic design mainly refers to the designer's reference to nature and the functional principles of the existence of natural substances, in-depth analysis of the function of the original form of natural objects and the relationship between the structure, and the combination with the form of natural objects, the synthesis of the performance in the design work.

### **2.2.3. Structural bionics**

Inspired by the outward morphological features of natural creatures, the tectonic relationships of organisms are equally inspiring to the artist. The way the whole or part of a creature is constructed and organized allows the artist to mimic its underlying similarities in order to create new images. For example, the stems and leaves of plants, and the forms, muscles, and bones of animals are objects of much study for artists.

## **3. Structural mechanics analysis in bionic sculpture art design**

### **3.1. Statue structural system**

#### **3.1.1. Structural force characteristics**

The main function of the background project of this paper is for people to visit, and its vertical load is only the self-weight of the structure, so the vertical bearing capacity of the structure has a large degree of richness. While the horizontal load caused by the structure side shift is relatively large, control of the horizontal side shift of the structure becomes the key of structural design. Horizontal lateral displacement

of the structure includes two parts: (1) the maximum displacement of the top of the structure, the value of which is too large to affect the normal use of the building, and (2) the inter-story displacement of the structure, the value of which is too large to damage the enclosure structure.

For frame structure, the lateral displacement generated by horizontal load consists of two parts: the first part is the lateral displacement caused by the bending deformation of beams and columns, the interstorey shear of the frame increases layer by layer from top to bottom, and the interstorey lateral displacement increases layer by layer from top to bottom, and the deformation curve of the whole structure is similar to that of the displacement curve caused by the shear deformation of cantilever members, so it is called “shear type”. Therefore, it is called “shear type”. The second part is the lateral displacement caused by the axial deformation of the column, under the action of horizontal load, due to the tension and compression of the column, the structure produces lateral displacement, and the lateral displacement between the layers decreases layer by layer from the top to the bottom, so that the structure is a “bending type” deformation. For frame structures, the first part of the lateral movement accounts for the main part of the total lateral movement, but with the increase of the height and aspect ratio of the structure, the second part accounts for more and more weight in the total lateral movement. The lateral movement of the apex caused by the axial deformation of the column is shown in the following equation:

$$u_N = \begin{cases} \frac{2}{3} \frac{V_0 H^3}{EAB^2} & \text{(Concentrated load at entry point)} \\ \frac{1}{4} \frac{V_0 H^3}{EAB^2} & \text{(Evenly distributed load)} \\ \frac{11}{30} \frac{V_0 H^3}{EAB^2} & \text{(Inverted triangle distribution load)} \end{cases} \quad (1)$$

In Equation (1),  $V_0$  is the total shear force generated at the bottom surface of the frame by the horizontal external load,  $E$  is the modulus of elasticity of the columns,  $A$  is the cross-sectional area of the columns,  $H$  is the height of the structure, and  $B$  is the distance between the outer columns.

### 3.1.2. Spatial finite element modeling

According to engineering experience, in the structural layout, for the outer ring along the curve direction of the edge of the beam, due to the direct bearing of the torque from the second external wall plate, the form of its cross-section should be used with good torsional performance of the closed cross-section, such as square steel pipe, round steel pipe, etc., should not be used in the angle or H-beam and other open cross-section. Between the nodes of the arrangement of the rod, should try to form a triangular geometric invariant system. After the completion of the structural arrangement of the plane in each layer, and then the vertical structure of the arrangement, that is, along the height of the body like the direction of the nodes connected to the plane of each layer. The basic vertical members are set up according to the column section, and H-beam, square steel pipe or round steel pipe can be used. Oblique members are set up according to the longitudinal support, usually using equal or unequal double angle steel section, can also use round steel pipe, square steel pipe or H-beam section. The connection between the bars is rigid connection.

### 3.2. Structural modal analysis

Modal analysis, also known as vibration mode superposition method of dynamic analysis, is the most commonly used and effective method for seismic analysis of linear structural systems [21]. Its main advantage lies in the fact that after calculating a set of orthogonal vectors, it can reduce a large set of overall equilibrium equations to a relatively small number of decoupled second-order differential equations, which significantly reduces the computational time used to solve these equations numerically. Modal analysis provides basic structural performance parameters that help this paper to make qualitative judgments about the structural response. Modal analysis provides relevant structural performance for structural-related static analyses, including structural static seismic action and static wind load action, and modal analysis is also the basis for other dynamic analyses (including response spectrum analysis and time course analysis).

#### 3.2.1. Modal analysis theory

For a system with  $n$  number of degrees of freedom, according to D'Alembert's principle, so that the internal and external forces on each mass are balanced, then the vibrational equilibrium equation of this system is  $n$  coupled equations [22]. In order to simplify the representation, the joint equations are often expressed in matrix form. The free vibration equation of the U-damped multi-degree-of-freedom system is:

$$[M]\{\ddot{y}\} + [K]\{y\} = \{0\} \quad (2)$$

where  $[M]$  denotes the mass matrix,  $[K]$  denotes the stiffness and array,  $\{\ddot{y}\}$  denotes the acceleration vector, and  $\{y\}$  denotes the displacement vector.

Let the solution of Equation (2) be:

$$\{y\} = \{\Phi\} \sin(\omega t + \phi_D) \quad (3)$$

In the formula,  $\omega$ —the circular frequency of vibration of the system, the  $\{\Phi\}$ —vector of displacement amplitude of the system, usually called the vibration mode vector:  $\phi_D$ —the initial phase angle. The expression for the mode vector  $\Phi$  is:

$$\{\Phi\} = \{\Phi_1, \Phi_2, \Phi_3 \dots \Phi_n\}^r \quad (4)$$

Substituting Equation (3) into Equation (2) yields the following equation:

$$(-\omega^2[M] + [K])\{\Phi\} = \{0\} \quad (5)$$

Since the right hand side of the equation is zero, Equation (5) is a multivariate chi-square equation. The condition that Equation (5) is also satisfied and the vibrational shape to though  $\{\Phi\}$  has a nonzero solution would be:

$$|-\omega^2[M] + [K]| = 0 \quad (6)$$

Equation (6) is an  $n$ -order joint equation with the circular frequency  $\omega$  as the unknown. This equation contains only the prime shortest matrix  $[M]$  and the stiffness matrix  $[K]$  of the system; therefore, the result of Equation (6) is called the characteristic equation of the system as it is determined only by the nature of the system itself and has nothing to do with the applied external loads. Here,  $\omega^2$  is called the eigenvalue of the system. By solving Equation (6),  $n$  different sizes of  $\omega$  values can be obtained, i.e.,  $\omega_1, \omega_2, \omega_3, \dots, \omega_n$ . If the value of each  $\omega$  already obtained is

substituted into Equation (5), the vibration vector  $\{\Phi_1\}, \{\Phi_2\}, \{\Phi_3\}, \dots, \{\Phi_n\}$  corresponding to each  $\omega$  can be obtained, which is called the 1st, 2nd, 3rd, ... and  $n$ th vibration vectors of the system, or vibration modes for short. In a multi-degree-of-freedom system, the number of vibration modes should be equal to the number of degrees of freedom of the system. If the system has  $n$  degrees of freedom, then there should be  $n$  vibration modes.

### 3.2.2. Modal analysis of a sculpture

**Table 1.** The first seven steps of the structure are ordered.

Vibration mode	Period (s)	Frequency (Hz)	Vibration description
1	1.0265	0.9848	Y direction movement
2	0.6544	1.5936	X direction movement
3	0.4788	2.1348	Y direction movement
4	0.4269	2.3815	X is slightly reversed
5	0.4197	2.4415	X direction
6	0.3948	2.5699	X is slightly torsional
7	0.3948	2.5699	X to move and reverse

SAP2000 provides two basic methods for modal decoupling, the eigenvector method and the Ritz vector method. The reason is that for large structural systems, solving the eigenvalue problem for free vibration modes and frequencies may require a large amount of computational work, and then simple eigenvector analysis may become difficult, and the spatial distribution of loads is completely ignored in the calculation of free vibration modes. Since many of the calculated shapes are orthogonal to the loads and do not participate in the dynamic response, the structural vibration shapes obtained with a lot of effort do not necessarily improve the accuracy of the calculations, or even do not help at all in some cases, which is the main problem of eigenvector analysis. However, in contrast, the Ritz vector method, because all the obtained eigenvectors are load-related, avoids the calculation of shapes that are not involved in the dynamic response, which is not helpful for the structural accuracy, and the limited computation time can be fully utilized in the calculation of shapes that are helpful for the accuracy of the results. In other words, with the same number of calculated shapes, the Ritz vector method will give more accurate results and higher structural mass participation factors as required by the code. The Chinese code stipulates that the number of calculated vibration modes should be such that the participating mass of the vibration modes is not less than 90% of the total mass. For seismic and wind loads, the response in horizontal direction is mainly considered, so if the cumulative value of the last vibration mode in X direction and Y direction is more than 0.9, it means that the number of vibration mode interception in the modal load condition meets the requirements of the code. In the modal analysis of a sculpture, the first 100 orders of vibration modes are calculated, in which the accumulation of horizontal vibration modes reaches more than 0.9, and the mass participation information shows that vertical vibration occurs in the 18th order of the structure, and the mass participation coefficient is 0.04, the participation coefficient of vertical vibration is relatively small, and the accumulation of horizontal vibration modes

reaches 0.9 at the same time, which indicates that the structure is mainly subjected to horizontal and torsional vibration, and the vertical vibration can be ignored. This indicates that the structure is dominated by horizontal and torsional vibration, and the vertical vibration can be neglected. The results of the first seven orders of modal analysis are shown in **Table 1**, and the period and frequency of the sixth and seventh orders are the same, which are 0.3948 s and 2.5699 Hz.

### 3.3. Analysis of calculation results

#### 3.3.1. Seismic effects analysis

In this paper, the seismic action analysis of the structure is carried out by using the vibration mode decomposition reaction spectrum method. For heterogeneous structures with uneven mass and stiffness distribution, the torsional coupling effect of the structure should be considered in the seismic analysis. The torsional coupling effect under bi-directional seismic action should be calculated according to the following equation:

$$S_{Ek} = \max \left\{ \sqrt{S_x^2 + (0.85S_y^2)}, \sqrt{S_y^2 + (0.85S_x^2)} \right\} \quad (7)$$

where:  $S_x, S_y$  is the unidirectional horizontal seismic effect in the  $X$  -direction and  $Y$  -direction, respectively.

The bearing reactions of typical bearing members under different seismic conditions are shown in **Table 2**. Because the structure itself is flexible and the structure is located in a geographic location with small seismic intensity, the bearing reaction force under different seismic conditions is very small, the largest bearing reaction force is B53, the seismic direction is the  $Y$ -direction, and the forces in the three directions are 0.2  $kN$ , 0.3  $kN$ , and 0.8  $kN$ , respectively. It can be seen that the seismic response of a sculpture structure is not obvious, and the seismic action can not be used as a control condition for the design of this sculpture.

**Table 2.** The support reaction of the typical support rod in different seismic direction.

Bar number	Seismic direction	$FX/kN$	$FY/kN$	$FZ/kN$
A34	X direction	0.15	0.2	0.2
	Y direction	0.15	0.2	0.2
	Bidirectional earthquake	0.1	0.1	0.3
A42	X direction	0	0.2	0.3
	Y direction	0.1	0.2	0.4
	Bidirectional earthquake	0.1	0.3	0.5
B47	X direction	0	0.1	0.1
	Y direction	0.1	0.15	0.2
	Bidirectional earthquake	0.15	0.2	0.5
B53	X direction	0.2	0.2	0.2
	Y direction	0.2	0.3	0.8
	Bidirectional earthquake	0.1	0.5	0.6

In finite element calculation, the loads acting on the model are categorized into three working conditions: gravity load,  $x$ -way wind load,  $y$ -way wind load,  $x$ -way seismic action, and  $y$ -way seismic action.

The gravity loads are calculated by simply entering the acceleration of gravity  $g$ , and the program automatically converts the body loads into equivalent nodal loads without manual intervention. It should be noted that the value of  $g$  is related to the units of length and force used in the modeling, and the units of length and force in this project are mm and N, respectively, accordingly  $g = 9800 \text{ N/mm}^2$ .

The wind loads acting on the structure in the actual project are surface loads, but since the elevations of the model are composed of curved surfaces, it is more difficult to apply surface loads directly on these surfaces. The model can be divided into several regions first, and then the wind load in each region is artificially converted into an equivalent nodal load directly applied to the key nodes in the region. This treatment has a certain effect on the local area of the node where the load is applied, but has no significant effect on the stress distribution pattern of the whole model.

ANSYS5.7 in the structure of the seismic role of the calculation need to first modal analysis of the model and on this basis according to the Chinese norms GBJ11-89 according to the II type of site 7 degrees of prevention of near-seismic input response spectral lines, the specific values are shown in **Figure 1**. In this project, seven vibration modes are taken for modal analysis and the maximum spectral value is 0.08549 when the damping ratio is 0.05 and the frequency is 4 Hz.

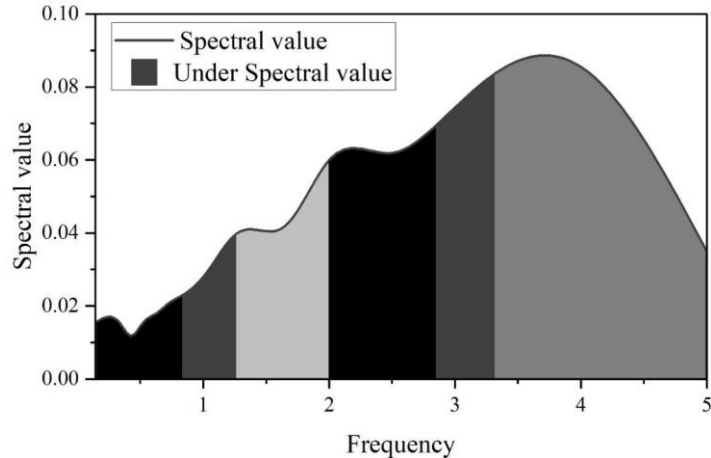


**Figure 1.** Reaction spectrum curve (Damping ratio = 0.05).

### 3.3.2. Stress checking of members

The ultimate load carrying capacity of the structure under all working conditions was modeled, and the results of the stress ratio envelope calculations for each unit are shown in **Figure 2**. Calculation results show that: under different working conditions, the maximum stress ratio of the cross-section strength of each member of a sculpture is 0.96987, and the strength of all members of the structure meets the design requirements.



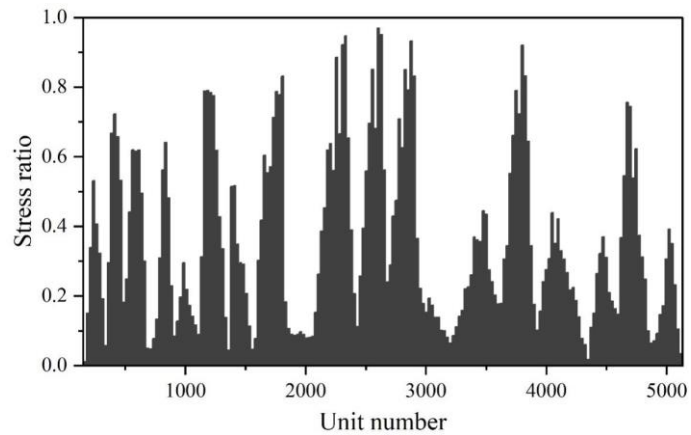


**Figure 2.** Stress ratio distribution of each element of the structure.

### 3.3.3. Overall stability analysis

The traditional design of regular steel structure usually adopts the length coefficient method, and the key of this analysis method is to determine the calculated length coefficient of the member, so as to determine the compressive stability coefficient of the member, and consider the influence of factors such as initial defects and residual stresses of the structure on the structural stability through the compressive stability coefficient. However, for shaped steel structures, determining the calculated length coefficients of members becomes a difficult problem in the design of steel structures. In order to solve this difficulty, methods based on the integration of nonlinear analysis and design have received international attention and made continuous development. As such a method that integrates the influence of various nonlinear factors, the direct analysis method can accurately simulate the deformation and instability characteristics of the structure during the analysis process, consider the mutual influence of each element, and do not need to carry out the calculation length estimation and stability check of each member. In this paper, the overall stability of the sculpture structure is analyzed based on the direct analysis method.

#### (1) Eigenvalue buckling analysis

Eigenvalue buckling analysis can reflect the stiffness of the structure under the specified loading conditions. Since the eigenvalue buckling analysis is based on the assumption of small deformation, the buckling factor obtained in this way can only provide a reference for the overall stability analysis of the structure. In the eigenvalue buckling analysis of a sculpture structure, the following three loading conditions are considered: (1) constant load + live load ( $1.0DL+1.0LL$ ), (2) constant load + wind load ( $1.0DL + 1.0W$ ), and (3) constant load + live load + wind load ( $1.0DL + 1.0LL + 1.0W$ ). **Figure 3** shows the eigenvalue buckling factor of the structure, and since buckling factor = buckling load/actual load, when the order is 5, the buckling factors for the three loading conditions are 208.5974, 114.1648, and 124.9748, respectively, and thus the structure has good overall stability.

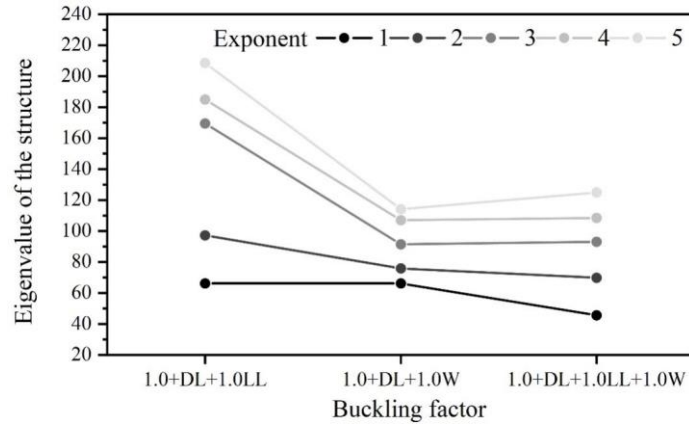


**Figure 3.** The characteristic value buckling factor of the structure.

(2) Nonlinear Buckling Analysis

In the direct analysis method, the overall defects of the structure and the initial defects of the members need to be considered. According to the “Steel Structure Design Standard”, the destabilization modes of the structure are roughly divided into two categories: frame-type structure destabilization and mesh-shell structure destabilization. According to the first-order buckling mode of this sculpture, the overall instability mode of the structure is mainly lateral instability, which is similar to that of the steel frame structure. Therefore, the overall defect magnitude of the structure is taken as  $H/250$  ( $H$  is the total height of the structure).

The value of initial deformation resulting from initial defects and residual gravitational forces in the member can be calculated by the following equation:

$$\delta_0 = e_0 \sin \frac{\pi x}{l} \tag{8}$$

where:  $\delta_0$  is the initial deformation value at  $x$  from the end of the member,  $l$  is the length of each segment when the member is produced,  $e_0$  is the initial deformation value at the central position of the member, and  $e_0$  in this project can be taken as  $l/400$ . Since there are many rods in this sculpture, and there are many kinds of initial deformation directions for each rod. If a member has  $N$  neighboring members, and the initial deformation direction is calculated once every  $45^\circ$ , the most unfavorable bearing capacity in all directions should be calculated by  $8^{n+1}$  times of envelope calculation, which is a huge amount of workload for this kind of calculation. Therefore, in order to simplify the calculation, the project carried out four directions of the envelope calculation, that is, the establishment of four members of the initial defect model for calculation.

**3.3.4. Force conditions**

A total of 18 pieces of strain gauges were placed on the surface of the reinforcement bars of the test model, and the strain distribution of each part of the test model under all levels of loading was obtained by organizing and analyzing the data of the strain gauges on the surface of the reinforcement bars, and the load-strain curves of some of the reinforcement measurement points are shown in **Figure 4**. When the test was loaded to about 160 kN, some of the steel bars had yielded, and the No. 12

bar's in the load to 160 kN, the steel structure began to yield, the strain was 150.4895  $\mu\epsilon$ , most of the members are close to the limit state.

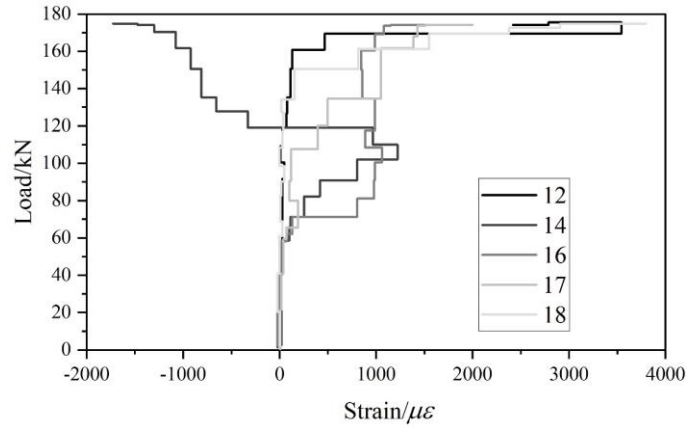


**Figure 4.** Tensile curve of steel bar.

**Table 3** shows the maximum positive and yz -plane shear stresses in various parts of the structure for the combined conditions compared to the material strength. The maximum positive stress of the structure is located in the connection area between A42 and B47, which is about 22.9364% of the material strength, and the maximum shear stress in the yz -plane is less than 10% of the material strength.

**Table 3.** Local construction of maximum positive stress and shear stress.

Bar part	Maximum positive stress		Plane shear stress	
	$\sigma_{max}$ (N/mm <sup>2</sup> )	$\frac{\sigma_{max}}{f_{yt}}$ (%)	$\tau_{yz}$ (N/mm <sup>2</sup> )	$\frac{\tau_{yz}}{f_{yv}}$ (%)
A34	14.5648	8.1685	7.0294	3.5198
A42	41.2696	22.9364	18.1765	9.1295
B47	5.2199	2.9158	3.1835	1.6495
B53	18.8265	10.5264	2.5678	1.3254
C64	16.7519	9.3285	4.5936	2.3965
C72	12.2639	6.8159	4.2165	2.1854
D35	13.1597	7.3688	3.9854	2.0639

Note:  $f_{yt} = 180 \text{ N/mm}^2, f_{yv} = 200 \text{ N/mm}^2$ .

**Figure 5** shows the period of the first seven vibration patterns in the structural modal analysis, for comparison, the figure also lists the results of SAP2000 calculations. As can be seen from the table, with ANSYS5.7 on a sculpture structure of the solid finite element modeling results, most of the period of each vibration mode is smaller than the rod model, vibration mode period of 1, ANSYS5.7 finite element analysis model under the cycle length of 0.5185 s, SAP2000 model for 0.5469 s.

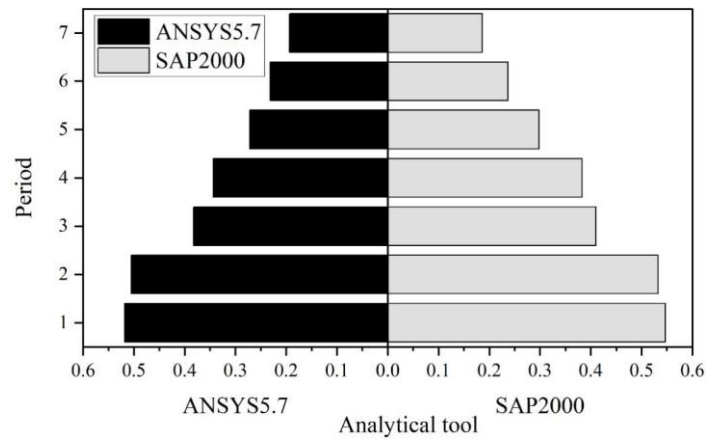


**Figure 5.** The period of the first seven oscillations in the structure modal analysis.

This is mainly due to the fact that the dimensional effects of each part of the structure are fully considered in the solid analysis, and the stiffness of the structure is increased compared with the rod model.

#### 4. Conclusion

In this paper, through the experimental simulation of the principle of biological system, after finishing, analyzing and then refining, we design a sculpture similar to the characteristics of the principle of biological system from three aspects: form, function and structure. Based on the force characteristics of the sculpture structure, a spatial finite element model is constructed to analyze the structural modes of the sculpture.

(1) The seismic analysis of the sculpture is carried out by using the vibration mode decomposition reaction spectrum method. Due to the good flexibility of the structure itself and the small seismic intensity of the geographic location where the structure is located, the bearing reaction forces under different seismic conditions are extremely small. The maximum bearing reaction force B53, the seismic direction is  $Y$  direction, the three directions of the force are  $0.2\text{ kN}$ ,  $0.3\text{ kN}$ ,  $0.8\text{ kN}$ , the sculpture structure is not obvious to the seismic response.

(2) Modal analysis is carried out according to the Chinese code, and the input response spectra of the 7-degree protection near-earthquake show that the maximum spectral value is  $0.08549$  when the damping ratio is  $0.05$  and the frequency is  $4\text{ Hz}$ .

(3) Calculate the ultimate bearing capacity of the sculpture components, bionic design of a sculpture cross-section strength of the maximum stress ratio of  $0.96987$ , the structure of all the components of the strength to meet the design requirements.

(4) The stiffness of the structure under the specified loading conditions is analyzed by eigenvalue buckling analysis, and when the order is  $5$ , the buckling factors under the three loading conditions are  $208.5974$ ,  $114.1648$ , and  $124.9748$ , respectively, and thus the structure has good overall stability.

In summary, based on the principle of structural dynamics, this paper analyzes the influence mechanism of factors such as the shape, mass distribution and connection mode of the sculpture structure on the vibration mode, and explains the relationship between the modal characteristics and the structural performance. Through the analysis of the overall stability of the structure, the weak link that affects the stability

of the structure is revealed. The bearing capacity of the whole structure can be significantly improved by adding a transverse partition beam in the sculpture. It can be seen from the nonlinear load-displacement curve that the sculpture structure has good ductility and local instability. In the future, the further analysis of the spatial effect of the sculpture structure is the focus of theoretical and experimental analysis in the future.

**Author contributions:** Conceptualization, JG and JZ; methodology, JG; software, JG; validation, JG and JZ; formal analysis, JG; investigation, JG; resources, JG; data curation, JG; writing—original draft preparation, JG; writing—review and editing, JG; visualization, JG; supervision, JG; project administration, JG; funding acquisition, JZ. All authors have read and agreed to the published version of the manuscript.

**Ethical approval:** Not applicable.

**Conflict of interest:** The authors declare no conflict of interest.

## References

1. Hsiao, K. W., Huang, J. B., & Chu, H. K. (2018). Multi-view wire art. *ACM Trans. Graph.*, 37(6), 242.
2. Yavuz, Ö. E. (2023). A study on the problem of meaning in the art of sculpture. *ArtGRID-Journal of Architecture Engineering and Fine Arts*, 5(2), 147-158.
3. Zhang, Y., Yu, X., & Cheng, Z. (2022). Research on the application of synthetic polymer materials in contemporary public art. *Polymers*, 14(6), 1208.
4. Farag, M. (2020). *Materials and processes of contemporary sculpture*. Cambridge Scholars Publishing.
5. Fu Guiyan. (2024). A Study on the Diversified Development Approaches of Sculpture Art Creation. *Journal of Management and Social Development*(4).
6. Drdácý, M., & Urushadze, S. (2023). Load Testing of Cultural Heritage Structures and Sculptures: Unconventional Methods for Assessing Safety. *Heritage*, 6(7), 5538-5558.
7. Zhu, Y. (2024). Integrating kinetic dynamics into sculpture and pottery for improved artistic form and structural stability. *Molecular & Cellular Biomechanics*, 21(2), 456-456.
8. Zetina Gargollo, C., Gomez Aguirre, A., & Ramirez Zamora, J. J. (2018, July). A Journey in Structural Geometry: Tensile Structures and Large Scale Sculptures. In *Proceedings of IASS Annual Symposia (Vol. 2018, No. 5, pp. 1-7)*. International Association for Shell and Spatial Structures (IASS).
9. Mostafa El-Sayed Mohamed Metwally, M. (2024). The Dynamics of Actual Movement and its Aesthetic Applications in The Field of Interactive Sculptural Formation. *International Journal of Advanced Research on Planning and Sustainable Development*, 7(1), 1-45.
10. Wang, Y. (2022). The interaction between public environmental art sculpture and environment based on the analysis of spatial environment characteristics. *Scientific Programming*, 2022(1), 5168975.
11. Imperial, R. (2023). Tension between Human and Nature in sculpture. *CAP-Public Art Journal*, 5(2), 8-25.
12. Dmitrievich, C. A. (2021). The pursuance of naturalness as one of the key trends in the sphere of modern wooden sculpture: domestic practice. *Culture and Art*, (6), 44-50.
13. Bank, D. J. (2021). *StickWork in Nature: Sculpture by Patrick Dougherty*. *Sculpture Review*, 70(1), 8-13.
14. Puppe, L., Jossberger, H., & Gruber, H. (2021). Creation processes of professional artists and art students in sculpting. *Empirical Studies of the Arts*, 39(2), 171-193.
15. Dmitrievich, C. A. (2022). Striving for naturalness as one of the key trends in the field of modern wooden sculpture: domestic practice. *SENTENTIA. European Journal of Humanities and Social Sciences*, (2), 28-33.
16. Li, N. (2024). The Micro Narrative Language Embodied by Shapes in Contemporary Sculpture Art. *Cultura: International Journal of Philosophy of Culture and Axiology*, 21(1).
17. March, P. L. (2024). What is an art experience like from the viewpoint of sculpting clay?. *Phenomenology and the Cognitive Sciences*, 1-27.

18. Smolina, O. O. (2019, December). Architecture and planning in arrangement of bionic pieces in modern urban landscape. In IOP Conference Series: Materials Science and Engineering (Vol. 687, No. 5, p. 055018). IOP Publishing.
19. Kurkowska, A. (2023). Bionic relations as features of the author's original concept of biomorphic plastic forms that belong to a place. *Architectus*, 113-121.
20. Anahar Nurul Aina, Muhammad Asyraf Muhammad Rizal, Muhamad Fauzi Abd Rased, Shukur Abu Hassan, Lin Feng Ng, Lakshminarasimhan Rajeshkumar... & Haris Ahmad Israr. (2024). Fiber-Reinforced Thermoplastic Composites for Future Use in Aircraft Radomes: Biomimetic Design Approaches and Its Performances. *Fibers and Polymers*(12),1-25.
21. Zeqiang Han, Hongwei Xia, Guan Wang & Guangcheng Ma. (2024). Prescribed modal vibration control and disturbance load analysis of rigid-flexible satellites. *Advances in Space Research*(11),5698-5712.
22. Xinheng Li, Pengbo Wang, Fan Yang, Xing Li, Yuxin Fang & Jie Tong. (2024). DAL-PINNs: Physics-informed neural networks based on D'Alembert principle for generalized electromagnetic field model computation. *Engineering Analysis with Boundary Elements*105914-105914.